EFFECTS OF INTERFACE PROPERTIES ON HORIZONTAL BACKFILL DEFORMATION AROUND WALL

Jing-Wen Chen[1], Nien-Hua Liu[2], and Jiun-Yaw Liou[3]

ABSTRACT

ABAQUS software, a Finite Element Method (FEM), is employed to study the behavior of deformation profiles of a horizontal backfill behind a vertical RC retaining wall. Mohr-Coulomb failure criterion is taken as yielding function and the associated flow rules are used in this study. The band zone of the maximum plastic strain contours is presented clearly in this research. From the quantification of the deformed profile in the backfill, wall friction angle plays an important role for passive lateral earth pressure rather than active lateral earth pressure. The potential failure sites on backfill surface, in active state, obtained by this study are 22.7% to 25.8% nearer to wall than that by traditional Coulomb's theory. On the contrary, they are 62.2% to 91.7% farther to wall in passive state. The potential failure site obtained by numerical analysis is closer to that obtained by Coulomb's theory as the wall is rougher both in active state and in passive state.

Key words: Deformed profile, backfill, retaining wall, ABAQUS.

1. INTRODUCTION

The earliest documentation concerning studies on retaining walls and backfill appeared in Coulomb's theory (1776), in which the lateral earth pressure is attained from the total-force-equilibrium point of view based on the wedge formed between the plane sliding face and a frictional retaining wall. Rankine's theory (1857), which applies only to a totally smooth and vertical back retaining wall, was released later; yet actual retaining walls are not smooth and frictionless. These analyses only satisfy force equilibrium conditions and have realistic limitations; however, they become popular in engineering practice due to their simplicity and ease. Terzaghi (1941) proposed the general wedge theory by assuming the failure surface as the arc of a logarithmic spiral. This paper will study the characters of potential failure from the viewpoint of deformed profile in the backfill. The sites of potential failure on the backfill surface are also compared to the traditional Coulomb's theory.

Roscoe (1970) conducted model tests on compacted sand and plotted contours for backfill shearing strain increment for researching development of soil rupture surfaces, images of dark bands of the specimens were also attained via X-ray applications. Roscoe indicated that soil in the dark bands had reached its critical state due to sufficient dilation, *i.e.*, by then the dilation rate should have reached zero. Sherif, *et al.* (1982) conducted both static and dynamic tests against dry Ottawa sand, finding that when the retaining wall moved away from the backfill to a cer-

tain extent and caused the backfill to enter into critical active or plastic failure state, then the friction between the retaining wall and backfill was deemed as reaching its maximum value. The timing of the plastic failure of the backfill could not yet be determined. Nakai (1985) adopted the extended concept of "Spatially Mobilized Plane" as the constitutive model of soil by using Finite Element Method (FEM) for considering different frictions between a retaining wall and the backfill. Within the zone with a defined safety factors ranging from 1.1 to 1.2, qualitative similarities were obtained with respect to both Coulomb's slip plane and Rankine's plastic wedge. Potts and Fourie (1986) analyzed embedded type retaining walls, 5 m in height and 1 m in width, using FEM and defined a failure zone with stress level greater than 0.99, fracture will develop from the base of the wall towards the backfill surface, which conformed with the position of a Rankine's plastic wedge. Bhatia and Bakeer (1989), based on experiments conducted by Matsuo, *et al.* (1978), performed numerical simulation analysis on a 10 m high RC basement wall of a building. The maximum principal stress difference $(\sigma_1 - \sigma_3)_{max}$ was taken to determine potential failure points in the backfill by this study. Fang, *et al.* (1994) conducted model tests on retaining wall in the situation of a translation, as the soil underneath the wall base move downward, the backfill above the wall base tended to move upward. The positions of cracks in the backfill surface are with a good agreement to the results derived by Terzaghi's theory. Day and Potts (1998) investigated the effects of interface properties on the behavior of a 5 m high and 0.2 m wide embedded wall when the active state and the passive state were developed respectively by FEM. The result revealed that there were areas of abrupt changes developed in both horizontal and vertical displacements of the backfill surface, and that positions of such areas were related to the wall friction angle between retaining wall and the backfill. From observations of the vector diagram of the backfill failure surface, the vector diagram appeared to be a plane surface of failure for smooth wall back, while the vector diagram appeared to be a curved surface of failure for rough wall back.

The study employs ABAQUS (2000) to simulate the translation behavior of a RC retaining wall. Since the actual failure of

Manuscript received October 20, 2006; revised February 26, 2007; accepted March 3, 2007.

[1] Professor (corresponding author), Department of Civil Engineering, National Cheng Kung University, Tainan City 701, Taiwan, R.O.C. (e-mail: geochen@mail.ncku.edu.tw)

[2] Lecturer, Department of Civil Engineering, Kao Yuan University, Lujhu Township, Kaohsiung County 82151, Taiwan, R.O.C. (e-mail: nhliu@cc.kyu.edu.tw); Ph.D. candidate, Department of Civil Engineering, National Cheng Kung University, Tainan City 701, Taiwan, R.O.C.

[3] Assistant Professor, Department of Civil Engineering, Kao Yuan University, Lujhu Township, Kaohsiung County 82151, Taiwan, R.O.C. (e-mail: ljy@cc.kyu.edu.tw)

the backfill are developed gradually, by the capability of setting up step-by-step parameters and conditions in the FEM, it is possible to observe and analyze variations in the deformed profile of the backfill, so as to be able to further control and comprehend the mechanism as well as to process the failure of a backfill.

2. METHOD OF STUDY

The retaining wall adopted in this study is 5 m high and 1m wide, with a horizontal sandy backfill, the layout of the wall and backfill is shown in Fig. 1.

Material properties and lateral earth pressure coefficient at rest are identical to the settings as Day and Potts (1998) adopted, such as elastic modulus $E = 60$ MPa, Poisson's ratio $\nu = 0.2$, effective cohesion $c' = 0$, effective internal friction angle $\phi' = 25°$, unit weight of soil $\gamma = 20$ kN/m^3 and lateral earth pressure coefficient at rest $K_0 = 1.0$. Other hypotheses include fully drained plane strain, fully associated flow rule and adoption of the Mohr-Coulomb failure criterion as the yielding function. In general, design strength of yielding strength of reinforced concrete f_c' = 21 MPa for a RC retaining wall is used. According to ACI Code (1999), the corresponding elastic modulus is $E = 2.13 \times 10^4$ MPa, Poisson's ratio and unit weight of RC are assumed $\nu = 0.17$ and $\gamma = 23.5$ kN/m^3, respectively. The simulated soil boundary to the right of the retaining wall is 40 m, while on the left is 15 m. The lowest layer of the soil boundary is 15 m away from the base of the retaining wall. The above mentioned distances are three to eight times the wall height H, therefore the boundary conditions of the soil body on all three sides are assumed to be roller bearing type, *i.e.*, the side boundaries are only allowed for vertical slides while the far end of the soil body is only allowed for to-and-fro movement; as for the other boundaries of the soil body, the boundary condition is assumed to be of traction free. In practice, RC retaining walls are mostly constructed in continued lengths, and the longitudinal scale is far greater than its height, therefore the numerical analysis based on the plane strain simulation not only is able to simplify the issue and shorten the calculation time, but it also conforms to the actual constructions on site. Grid seeds are created at the beginning, manually using the ABAQUS/CAE Preprocessor, the two-dimensional grid as shown in Fig. 2 is subsequently established by way of auto-meshing.

Both the retaining wall and soil body employ the plane strain elements of a 8-node quadrilateral (CPE8R), the back and the base of the retaining wall are taken as contact elements with the soil body, normal direction of the contact faces select the Hard Contact item, with Penalty item for the tangent direction. The Mohr-Coulomb failure criterion is as $\tau' = \mu \cdot \sigma'$, where τ' is the effective shearing strength, σ' is the effective normal stress, μ = tan ϕ', is equal to the internal friction coefficient of the soil body and ϕ' is the effective internal friction angle. The friction between the wall and the backfill, which is setting equal to the wall friction angles of the backfill are $\delta = 0$, $\delta = 12.5°$, $\delta = 17.5°$, and $\delta = 25°$, respectively.

The Step Module of ABAQUS is used for simulating the translation process of the retaining wall. The lateral earth pressure coefficient at rest K_0 was adjusted to 1.0 firstly, and then an increase in the wall translation towards the backfill was simulated for the process of reaching the passive state; to the contrary, an increase in the wall translation away from the backfill was simulated for the process of reaching the active state.
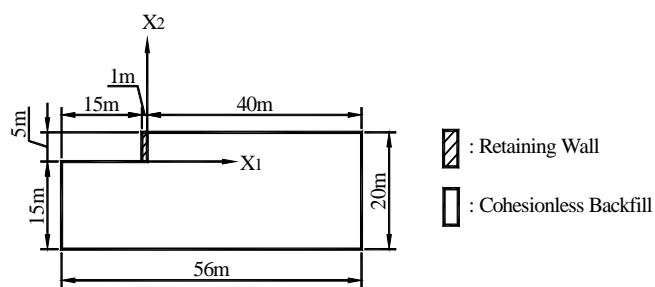
Fig. 1   A retaining wall and the horizontal type backfill
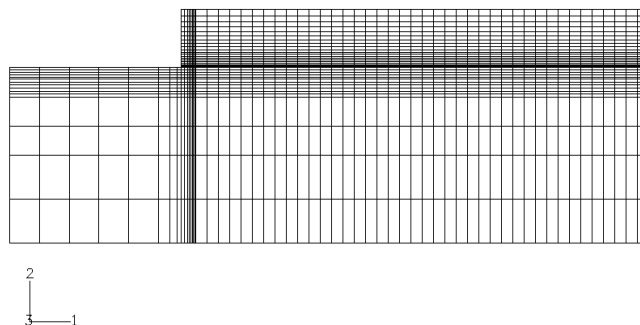
Fig. 2   A two-dimensional ABAQUS simulation analysis grid

Using the Visualization Module in the ABAQUS software, analysis results such as grid coordinates x_1 and x_2, horizontal displacement u_1, vertical displacement u_2, displacement u, and maximum plastic strain ε_{max}^p are saved as editable data files. With the numerical data of the backfill, contours associated with each step of the translation process can be created with the analytic or drafting software, for instance, the contour of a displacement and the contour of the maximum plastic strain corresponding to a specific wall displacement S under active or passive process. Results of the analysis are discussed in the following section.

3. NUMERICAL RESULTS AND DISCUSSIONS

3.1   Distribution of Backfill Displacements

Simulating the translation process in which a retaining wall moves away from or toward the backfill, enables the backfill to gradually enter into active or passive state. Analyses are conducted for the variation of displacement and maximum plastic strain in the backfill under four conditions of wall friction angle δ.

The displacements u of the node in the backfill corresponding to a specific wall displacement S can be retrieved to plot the contour of the backfill displacement u. The contours of displacements u under the active state, with $\delta = 0$ and $S = -145$ mm is shown in Fig. 3(a). The displacement is increasing as it is much closer to the wall. The contour of displacements u under the passive state with $\delta = 0$ and $S = 215$ mm is shown in Fig. 3(b). As same tendency as under the active state, the displacement u is larger as it is closer to the wall. At the same displacement u, the distance to the wall is larger under the passive state than that under the active state. The tendencies on both the active state and passive state agree with that evaluated by Coulomb's theory.
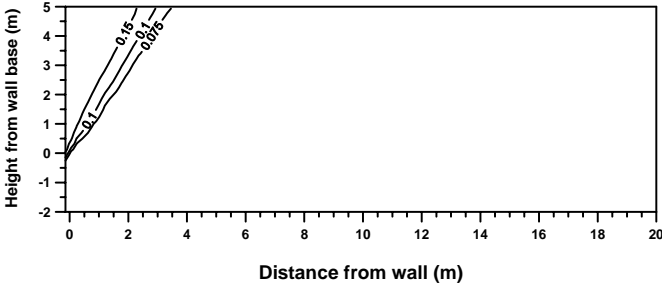
Fig. 3(a) Displacement contour of backfill in the active state ($\delta = 0$, $S = -145$ mm)
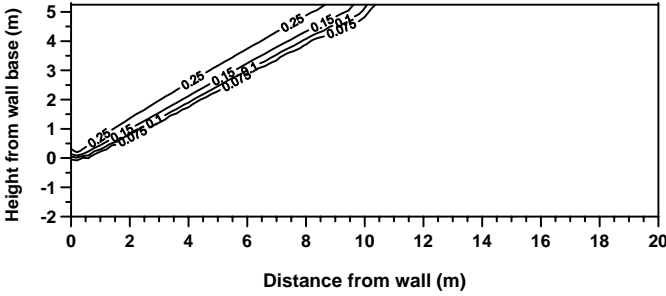
Fig. 3(b) Displacement contour of backfill in the passive state ($\delta = 0$, $S = 215$ mm)

In order to describe a certain displacement u in the backfill corresponding a specific displacement of the wall S. Define D_u as the distance from the retaining wall to an intersection, which is formed by the backfill surface and the contour in correspondence to a certain u, then normalize S and D_u with height of the wall H, such that S/H and D_u/H values become dimensionless. Figures 4(a) and 4(b) are the compilation of distribution of backfill displacements in active process and passive process respectively.

In active process D_u value increases as the wall displacement increases can be found in Fig. 4(a). Under identical S values, D_u value corresponding to $u = 100$ mm is smaller than that to $u = 75$ mm. This indicates that displacement u of the backfill increases when the distance of the backfill from the back of the retaining wall decreases. In the initial stage when the retaining wall starts to translate away from the backfill, the relationship between D_u and the wall friction angle δ is irregular until $S/H \leq -0.013$ ($u = 75$ mm) or $S/H \leq -0.021$ ($u = 100$ mm) is reached; after that, D_u increases when δ increases, but all the D_u values are smaller than height of the retaining wall H.

In passive process D_u value increases as the wall displacement increases can also be found in Fig. 4(b). Under identical S values, the D_u value corresponding to $u = 100$ mm is smaller than that to $u = 75$ mm. This also indicates that displacement of the backfill increases when the distance of the backfill from the back of the retaining wall decreases. In the initial stage when the retaining wall starts to translate towards the backfill, the relationship between D_u and the wall friction angle δ is irregular until $S/H \geq 0.021$ ($u = 75$ mm) or $S/H \geq 0.025$ ($u = 100$ mm) is reached; D_u increases when δ increases. After $S/H \geq 0.021$, all D_u values are greater than H values despite $\delta = 0$, $\delta = 12.5°$, $\delta = 17.5°$ or $\delta = 25°$.
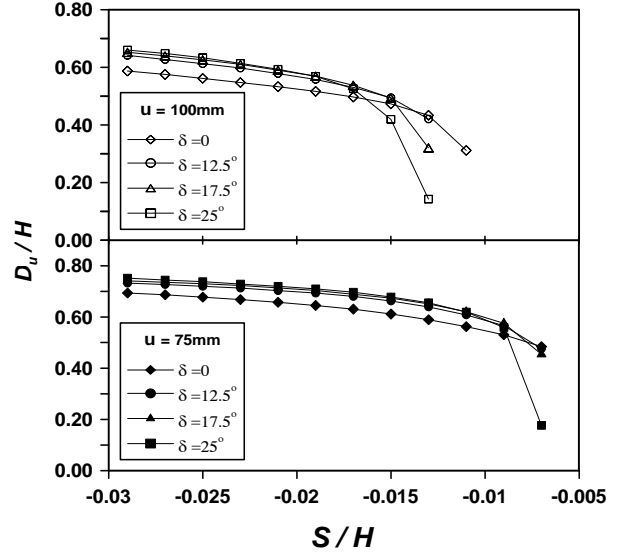
Fig. 4(a) Function of backfill D_u/H vs. S/H in active process
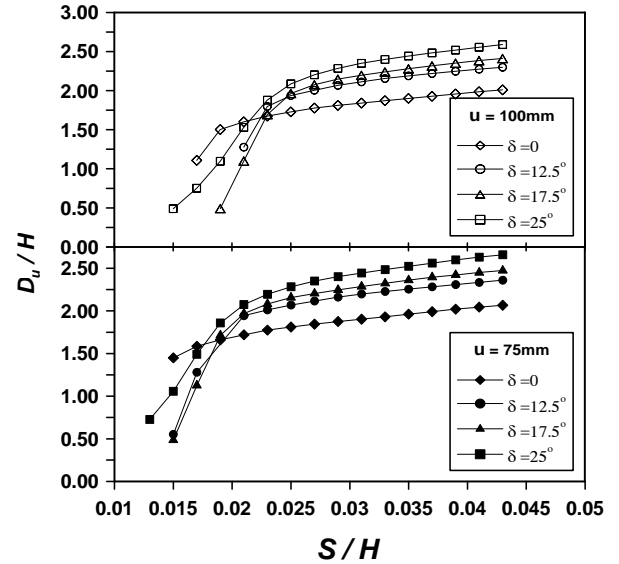
Fig. 4(b) Function of backfill D_u/H vs. S/H in passive process

3.2 Distribution of Maximum Plastic Strain of Backfill

The maximum plastic strain ε_{max}^p of the node in the backfill corresponding to a specific wall displacement S can be retrieved to plot the contour of the backfill maximum plastic strain ε_{max}^p. The contours of maximum plastic strain ε_{max}^p under the active state with $\delta = 0$ and $S = -145$ mm are shown in Fig. 5(a). In the figure the contour of ε_{max}^p develops upwards from the base of the retaining wall to the right of the backfill and forms a band zone enclosed by the left and right contours of the same ε_{max}^p value. The smaller the value of ε_{max}^p is, the wider the band zone gets. The contours of maximum plastic strain ε_{max}^p under the passive state with $\delta = 0$ and $S = 215$ mm are shown in Fig. 5(b). The contour of ε_{max}^p also develops upwards from the base of the retaining wall to the right of the backfill and forms a band zone enclosed by the left and right contours. The smaller the value of ε_{max}^p is, the wider the band zone becomes, too.
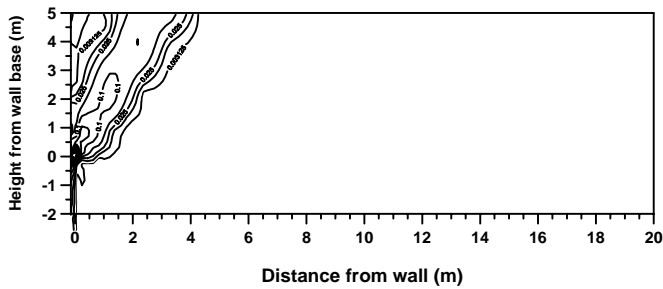
Fig. 5(a) **Maximum plastic strain contour of backfill in the active state ($\delta = 0$, $S = -145$ mm)**
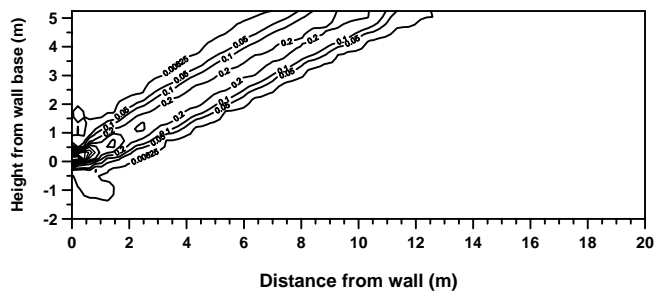
Fig. 5(b) **Maximum plastic strain contour of backfill in the passive state ($\delta = 0$, $S = 215$ mm)**

For indicating this band zone, define C_ε as the distance from the retaining wall to the center point of two intersections. These two intersections represent the crossing point of the left contour from the band zone with the backfill surface, as well as the crossing point of the right contour from the band zone with the backfill surface, in correspondence to a certain ε^p_{max}. Define D_ε as the distance from the retaining wall to an intersection, which is formed by the backfill surface and the right contour from the band zone in correspondence to a certain ε^p_{max}. The compilation of C_ε with $\varepsilon^p_{max} = 0.025$ and D_ε with $\varepsilon^p_{max} = 0.003125$ under the active process is shown in Fig. 6(a). Likewise, the compilation of C_ε with $\varepsilon^p_{max} = 0.05$ and D_ε with $\varepsilon^p_{max} = 0.00625$ under the passive process is shown in Fig. 6(b). The same normalizations are conducted for S, C_ε, and D_ε with height of the wall H, so that S/H, C_ε/H and D_ε/H become dimensionless.

In Fig. 6(a), it shows that, in active process, in the initial stage when the retaining wall starts to translate, the relationship between D_ε and the wall friction angle δ is irregular; after reaching $S/H \le -0.009$, D_ε increases when δ increases, and after $S/H \le -0.011$, C_ε increases when δ increases; but in any stage of the translation process, C_ε and D_ε values are all smaller than the retaining wall height H.

Observing the passive process in Fig. 6(b), after reaching $S/H \ge 0.007$, D_ε increases when δ increases; while after $S/H \ge 0.017$, C_ε also increases when δ increases. Furthermore, after $S/H \ge 0.007$ or $S/H \ge 0.017$, the corresponding D_ε and C_ε values are all greater than H values whether the contact surface between retaining wall and backfill is smooth or rough.
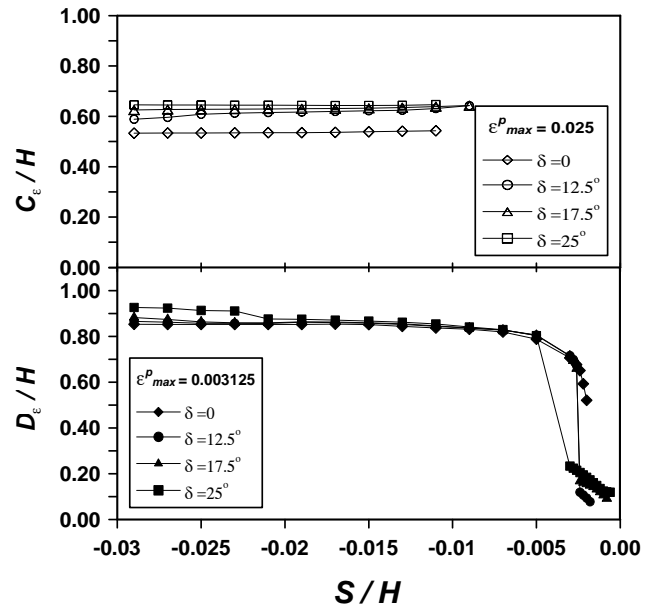
Fig. 6(a) **Function of backfill C_ε/H and D_ε/H vs. S/H in active process**
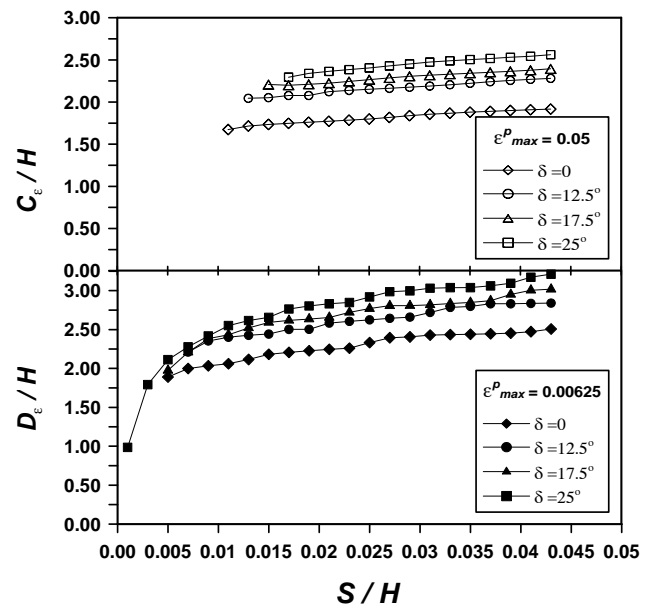
Fig. 6(b) **Function of backfill C_ε/H and D_ε/H vs. S/H in passive process**

3.3 Potential Failure Site on Backfill Surface

The displacements and the maximum plastic strain of backfill, discussed in above sections, may be taken as potential failure sites from the viewpoint of displacement field. Analyses are conducted for the variation of the displacements and the maximum plastic strain in the backfill under four conditions of wall friction angle δ in three displacement steps, respectively $S = -105$ mm, $S = -125$ mm, and $S = -145$ mm for active process; $S = 105$ mm, $S = 125$ mm, and $S = 215$ mm for passive process. In order to compare the numerical results with that calculated by Coulomb's theory, define D_{CT} as the distance from the retaining

wall to an intersection, which is formed by a failure plane analyzed by Coulomb's theory. The intersection formed by a failure plane analyzed by Coulomb's theory, with the backfill surface to the back of the retaining wall. Conducting normalization to D_u, C_ε, and D_{CT} with wall height H, D_u/H, C_ε/H and D_{CT}/H values become dimensionless. The corresponding compared results for active process and passive process are shown in Table 1 and Table 2 separately.

From Table 1, it shows that values of both D_u/H and C_ε/H are all smaller than that of D_{CT}/H for any δ value under active process. Contrarily in Table 2, it may be seen that values of both D_u/H and C_ε/H are all larger than that of D_{CT}/H for any δ value under passive process. The results indicate that the distances between the potential failure sites on backfill surface and the wall in active process, obtained by numerical analysis are all shorter than that by traditional Coulomb's theory. In passive process, the distances from the potential failure sites on backfill surface to the wall calculated by numerical analysis are all longer than that by traditional Coulomb's theory.

In order to provide a quantitative detail of the distance of the potential failure site calculated by numerical analysis and Coulomb's theory with different wall friction angle δ, the values of D_u and D_{CT} are compared through the formula $(D_u - D_{CT})/D_{CT}$. From Table 1, when $\delta = 0$, $S = -145$ mm, then $(D_u - D_{CT})/D_{CT} = -0.258$. When $\delta = 25°$, $S = -145$ mm, then $(D_u - D_{CT})/D_{CT} = -0.227$. The results show that the absolute value of $(D_u - D_{CT})/D_{CT}$ will decrease when the value of δ increases. That is to say, the potential failure site obtained by numerical analysis is closer to that obtained by Coulomb's theory as the wall is rougher in active state. From Table 2, when $\delta = 0$, $S = 215$ mm, then $(D_u - D_{CT})/D_{CT} = 0.917$. When $\delta = 25°$, $S = 215$ mm, then $(D_u - D_{CT})/D_{CT} = 0.622$. The results show that the value of $(D_u - D_{CT})/D_{CT}$ will also decrease when the value of δ increases. In other words, the potential failure site obtained by numerical analysis is also closer to that obtained by Coulomb's theory as the wall is rougher in passive state.

3.4 Band Length and Band Width of the Maximum Plastic Strain Zone

The same approach, as above section, is taken for analyzing the maximum plastic strain by developing the contour upwards to the right from the base of the retaining wall and forming a band zone enclosed by the contours on the left and right, then the relative position of the zone is represented by the center point of the left and right contours. In active process, the band zone with $\varepsilon_{max}^p = 0.025$ is analyzed. The length of the line linking the center point on the backfill surface and base of the retaining wall is defined as length L of the maximum plastic strain band. Perpendicular lines are made to the left and right contours for estimating the band width, which is then defined as width W of the maximum plastic strain band. Normalization is conducted to both L and W, so as to obtain dimensionless L/H and W/H. Figure 7(a) is the compilation of the length and width of the maximum plastic strain band. Likewise in passive process, the band zone analysis is conducted by taking $\varepsilon_{max}^p = 0.05$, the results are shown in Fig. 7(b).

Table 1   **Comparison of potential failure site in active process ($u = 75$ mm, $\varepsilon_{max}^p = 0.025$)**

S (mm)	$D_u/H\ (C_\varepsilon/H)$			
	$\delta = 0$ $D_{CT}/H = 0.93$	$\delta = 12.5°$ $D_{CT}/H = 0.96$	$\delta = 17.5°$ $D_{CT}/H = 0.96$	$\delta = 25°$ $D_{CT}/H = 0.97$
−105	0.66 (0.54)	0.70 (0.62)	0.71 (0.63)	0.72 (0.64)
−125	0.68 (0.53)	0.72 (0.61)	0.73 (0.63)	0.74 (0.65)
−145	0.69 (0.53)	0.73 (0.59)	0.74 (0.63)	0.75 (0.65)

Table 2   **Comparison of potential failure site in passive process ($u = 75$ mm, $\varepsilon_{max}^p = 0.05$)**

S (mm)	$D_u/H\ (C_\varepsilon/H)$			
	$\delta = 0$ $D_{CT}/H = 1.08$	$\delta = 12.5°$ $D_{CT}/H = 1.28$	$\delta = 17.5°$ $D_{CT}/H = 1.40$	$\delta = 25°$ $D_{CT}/H = 1.64$
105	1.72 (1.77)	1.94 (2.12)	1.97 (2.23)	2.07 (2.36)
125	1.81 (1.80)	2.07 (2.15)	2.16 (2.27)	2.28 (2.41)
215	2.07 (1.92)	2.36 (2.28)	2.47 (2.39)	2.66 (2.56)
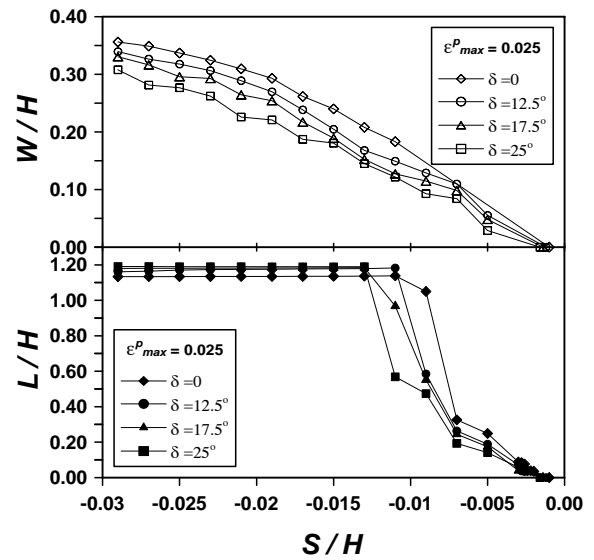
Fig. 7(a)   **Function of backfill *W/H* and *L/H* vs. *S/H* in active process**
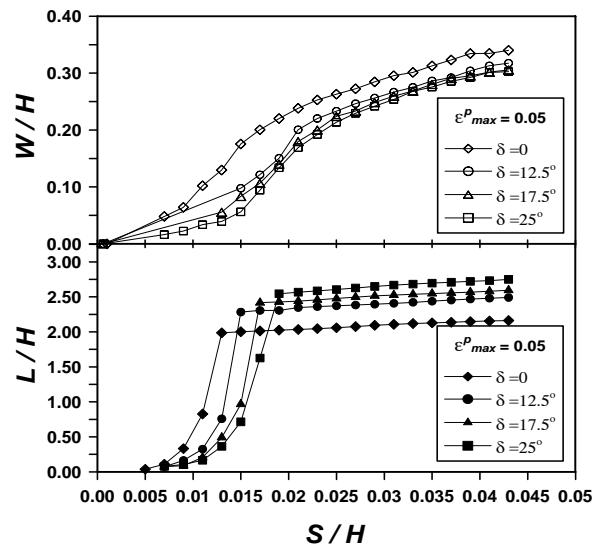
Fig. 7(b)   **Function of backfill *W/H* and *L/H* vs. *S/H* in passive process**

From Fig. 7(a), it shows that under active process, length *L* and width *W* of the maximum plastic strain band increase when the wall displacement increases. At the beginning stage of the translation process, under identical wall displacements *S*, *L* value generally decreases when the wall friction angle δ increases. Only after $S/H \leq -0.013$, *L* value increases when the wall friction angle δ increases; but the differences between the corresponding *L* values are insignificant, for example, when $S/H = -0.029$, *L/H* values are between 1.13 and 1.19. This reflects that the wall friction angle δ is insignificant to the horizontal active lateral earth pressure. As for *W* values, at the beginning stage of the translation process, under identical *S* values, the relationship is constant as the *W* value decreases when the wall friction angle δ increases. As $S/H = -0.029$, *W/H* changes from 0.36 to 0.31.

In Fig. 7(b), it indicates that as both *L* and *W* of the maximum plastic strain band increase, the wall displacement increases. At the beginning stage of the translation, under identical wall displacements *S*, *L* value generally decreases when the wall friction angle δ increases. Only after $S/H \geq 0.019$, *L* value increases when the wall friction angle δ increases, and the differences between the corresponding *L* values are significant, for example when $S/H = 0.043$ *L/H* values are between 2.16 and 2.75. This reflects that the wall friction angle δ is significant to the horizontal passive lateral earth pressure. As for *W* values, at the beginning stage of the translation process, under identical *S* values, the relationship is constant as the *W* value decreases when the wall friction angle δ increases. As $S/H = 0.043$, *W/H* changes from 0.34 to 0.30.

4. CONCLUSIONS

From the quantification of the deformed profile in the backfill, it is revealed that the wall friction angles are insignificant to the horizontal active lateral earth pressure; nevertheless, the wall friction angles are significant to the horizontal passive lateral earth pressure. The above results are agreed to the variation based on the traditional Coulomb's theory. The band zone of potential failure surfaces is presented clearly in this study. The potential failure sites on backfill surface, in active state, obtained by numerical analysis are 22.7% to 25.8% nearer to wall than that by Coulomb's theory in active state. In passive state, the potential failure sites on backfill surface calculated by numerical analysis are 62.2% to 91.7% farther to wall than that by Coulomb's theory in passive state. The potential failure site obtained by numerical analysis is closer to that obtained by Coulomb's theory as the wall is rougher both in active state and in passive state.

REFERENCES

ABAQUS (2000). *ABAQUS User's Manual* (*Version 6.1*), Hibbitt, Karlsson, Sorensen, Inc., Pawtucket, U.S.A.

ACI Committee 318 (1999). *Building Code Requirements for Structural Concrete* (*ACI318-99*) *and Commentary* (*ACI 318R-99*), American Concrete Institute, Detroit.

Bhatia, S. K. and Bakeer, R. M. (1989). "Use of the finite element method in modelling a static earth pressure problem." *International Journal for Numerical and Analytical Methods in Geomechanics*, 13, 207−213.

Coulomb, C. A. (1776). *Essai sur une Application des Regles de Maximis et Minimum a quelques Problemes de Statique Relatifs a l'Architecture*, Mem. Acad. Roy. des Sciences, Paris, 3, 38.

Day, R. A. and Potts, D. M. (1998). "Short communication the effect of interface properties on retaining wall behaviour." *International Journal for Numerical and Analytical Methods in Geomechanics*, 22, 1021−1033.

Fang, Y. S., Chen, T. J., and Wu, B. F. (1994). "Passive earth pressures with various wall movements." *Journal of Geotechnical Engineering*, ASCE, 120(8), 1307−1323.

Matsuo, M., Kenmochi, S., and Yagi, H. (1978). "Experimental study on earth pressure of retaining walls by field tests." *Soils and Foundations*, 18(3), 27−41.

Nakai, T. (1985). "Finite element computations for active and passive earth pressure problems of retaining wall." *Soils and Foundations*, 25(3), 98−112.

Potts, D. M. and Fourie, A. B. (1986). "A numerical study of the effects of wall deformation on earth pressures." *International Journal for Numerical and Analytical Methods in Geomechanics*, 10, 383−405.

Rankine, W. J. M. (1857). "On the stability of loose earth." *Philosophic Transactions of Royal Society*, London, Part I, 9−27.

Roscoe, K. H. (1970). "The influence of strains in soil mechanics." *Geotechnique*, 20(2), 129−170.

Sherif, M. A., Ishibashi, I., and Lee, C. D. (1982). "Earth pressure against rigid retaining walls." *Journal of Geotechnical Engineering Division*, ASCE, 108(5), 679−695.

Terzaghi, K. (1941). "General wedge theory of earth pressure." *Transactions*, ASCE, 106, 68−97.